

Supporting Information

A robust network 1 binder with dual functions of Cu²⁺ ions as ionic crosslinking and chemical binding agents for highly stable Li–S batteries

Jie Liu,^{a,c,‡} Minghao Sun,^{c,‡} Qian Zhang,^b Feifei Dong,^a Payam Kaghazchi,^b Yanxiong Fang,^a Shanqing Zhang^{d,*} and Zhan Lin^{a,c,*}

^a*School of Chemical Engineering and Light Industry, Guangdong University of Technology, Guangzhou 510006, China*

E-mail: zhanlin@gdut.edu.cn

^b*Physikalische und Theoretische Chemie, Institut für Chemie und Biochemie, Freie Universität Berlin, Berlin 14195, Germany*

^c*Zhejiang Provincial Key Laboratory of Advanced Chemical Engineering Manufacture Technology, College of Chemical and Biological Engineering, Zhejiang University, Hangzhou 310027, China*

^d*Centre for Clean Environment and Energy, Environmental Futures Research Institute and Griffith School of Environment, Gold Coast Campus, Griffith University, QLD 4222, Australia*

E-mail: s.zhang@griffith.edu.au

*Corresponding authors.

‡These authors contribute equally to this work.

Table S1 Comparisons of capacity retention rates of sulfur electrodes in binder-related studies.

Reference	Binder	Current density	Cycle number	Capacity (mAh g ⁻¹)	Retention rate ¹
This work	SA-Cu6	0.2 C	100	925	83%
1	Reduced graphene oxide-polyacrylic acid	0.5 C	100	635	77%
2	Poly(vinylidene difluoride-trifluoroethylene)	0.2 C	100	801	~67%
3	Sodium alginate	0.2 C	50	508	65%
4	LA132	0.2 C	50	885	76%
5	Gelatin	0.4 mA cm ⁻²	50	408	36%
6	Mixture of SBR and CMC	100 mA g ⁻¹	60	580	67% ²
7	Gum arabic	0.2 C	50	1090	79%
8	Perylene bisimide/PVDF composite	1.0 C	150	600	86%
9	Carbonyl-β-cyclodextrin β-cyclodextrin with a quaternary ammonium cation	0.2 C	50	1456	~77%
10		100 mA g ⁻¹	100	928	67%

¹Retention rate is computed for the initial discharge capacity. Some studies without the initial discharge capacity are not listed.

²Retention rate is computed for the capacity of the 5th cycle.

Table S2 Comparisons of sulfur loadings of different sulfur electrodes in binder-related studies showing that using SA-Cu6 binder can achieve high-loading electrode.

Reference ³	Binder	Sulfur loading (mg cm ⁻²)
This work	SA-Cu6	8.05
20	Carbonyl-β-cyclodextrin	3.0
43	Mixture of PAA and poly(3,4-ethylenedioxythiophene) : poly(styrenesulfonate)	0.8
44	Polyamidoamine dendrimers	4.4
45	LA132	1.0
46	Reduced graphene oxide-polyacrylic acid	0.8
47	Perylene bisimide/PVDF composite	1.0
48	Polypyrrole and polyurethane nanocomposite	4.6
49	Amino functional group binder	8.0
50	Cross-linked CMC-citric acid	14.9
51	Polymerization of hexamethylene diisocyanate with ethylenediamine	0.5
52	PEO ₁₀ LiTFSI	4.0
53	PEO:PVP	5.26
54	Polyethylenimine	8.6
55	Polydiallyldimethylammonium	3.0

³References are listed in the maintext.

References:

- 1 G. Xu, Q. Yan, A. Kushima, X. Zhang, J. Pan, J. Li, *Nano Energy* **2017**, *31*, 568.
- 2 H. Wang, V. Sencadas, G. Gao, H. Gao, A. Du, H. Liu, Z. Guo, *Nano Energy* **2016**, *26*, 722.
- 3 W. Bao, Z. Zhang, Y. Gan, X. Wang, J. Lia, *J. Energy Chem.* **2013**, *22*, 790.
- 4 X. Hong, J. Jin, Z. Wen, S. Zhang, Q. Wang, C. Shen, K. Rui, *J. Power Sources* **2016**, *324*, 455.
- 5 J. Sun, Y. Huang, W. Wang, Z. Yu, A. Wang, K. Yuan, *Electrochim. Acta* **2008**, *53*, 7084.
- 6 M. He, L. X. Yuan, W. X. Zhang, X. L. Hu, Y. H. Huang, *J. Phys. Chem. C* **2011**, *115*, 15703.
- 7 G. Li, M. Ling, Y. Ye, Z. Li, J. Guo, Y. Yao, J. Zhu, Z. Lin, S. Zhang, *Adv. Energy Mater.* **2015**, *5*, 1500878.
- 8 P. D. Frischmann, Y. Hwa, E. J. Cairns, B. A. Helms, *Chem. Mater.* **2016**, *28*, 7414.
- 9 J. Wang, Z. Yao, C. W. Monroe, J. Yang, Y. Nuli, *Adv. Funct. Mater.* **2013**, *23*, 1194.
- 10 F. Zeng, W. Wang, A. Wang, K. Yuan, Z. Jin, Y. Yang, *ACS Appl. Mater. Inter.* **2015**, *7*, 26257.

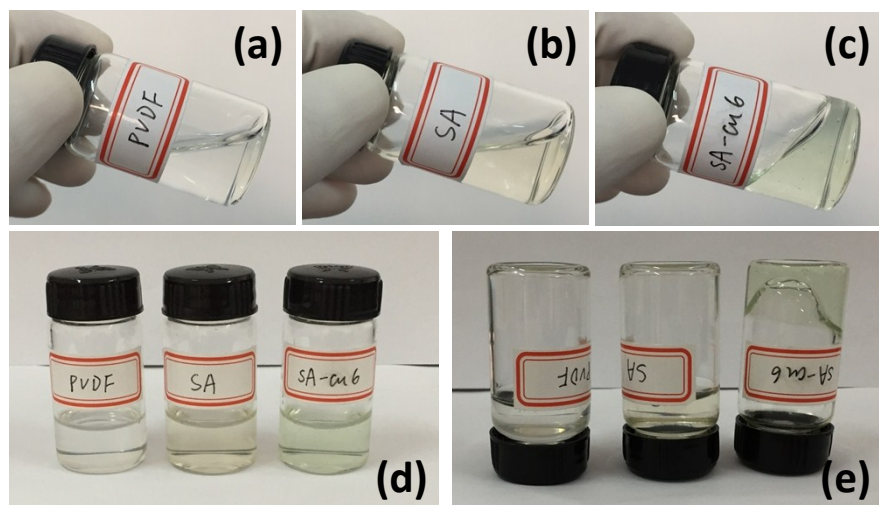


Fig. S1 Photos of (a) PVDF binder, (b) SA binder, (c) SA-Cu6 binder, (d) erected binders, and (e) inverted binders, visually demonstrating the cross-linking effect of SA and Cu²⁺ ions.

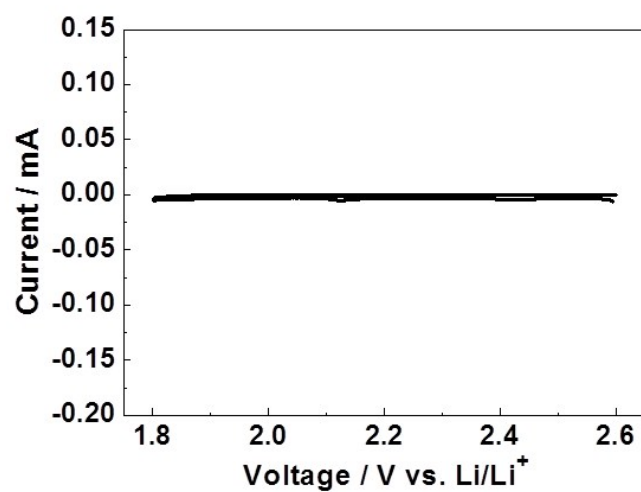


Fig. S2 CV curves of SA-Cu6 binder at 0.1 mV s⁻¹. The electrode consists of SA-Cu6 binder and super P conductive additive with a mass ratio of 1:1.

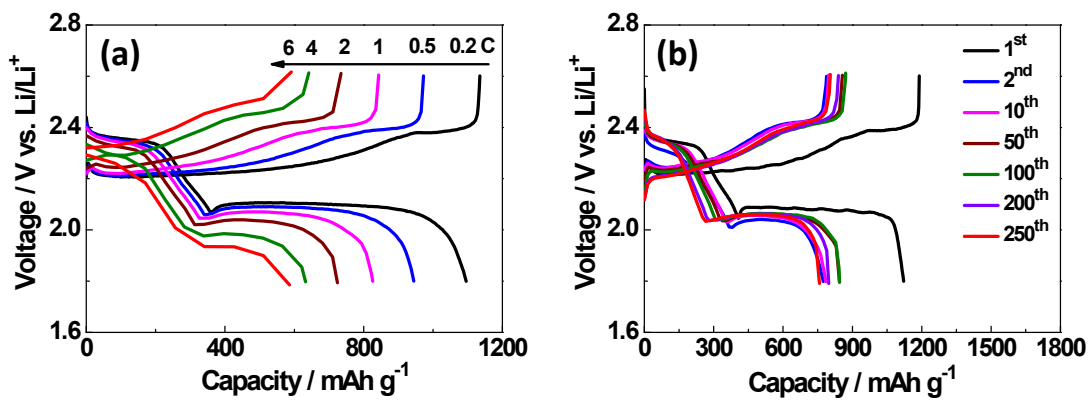


Fig. S3 Charge-discharge curves of S@SA-Cu6 electrodes (a) at different rates and (b) at 1 C for different cycles (the first cycle is at 0.2 C).

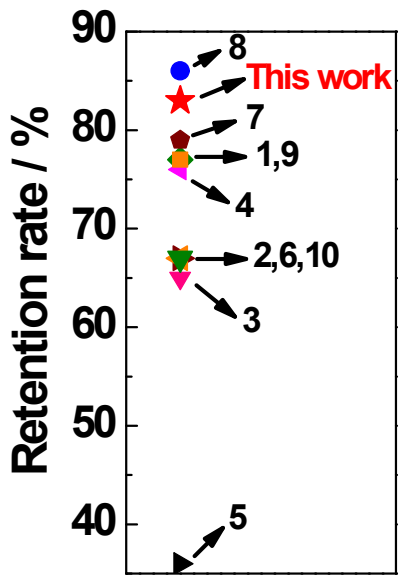


Fig. S4 Comparisons of capacity retention rates of sulfur electrodes in binder-related studies, according to Table S1.

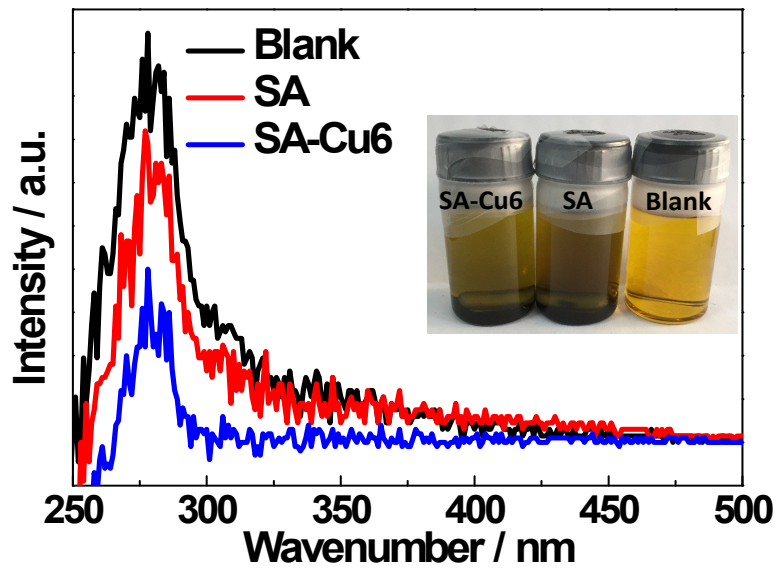


Fig. S5 UV-vis spectra of SA-Cu6/super P and SA/super P soaking in 2 mM Li₂S₆ solutions and pristine 2 mM Li₂S₆ solution, the inset is digital image of these solutions.

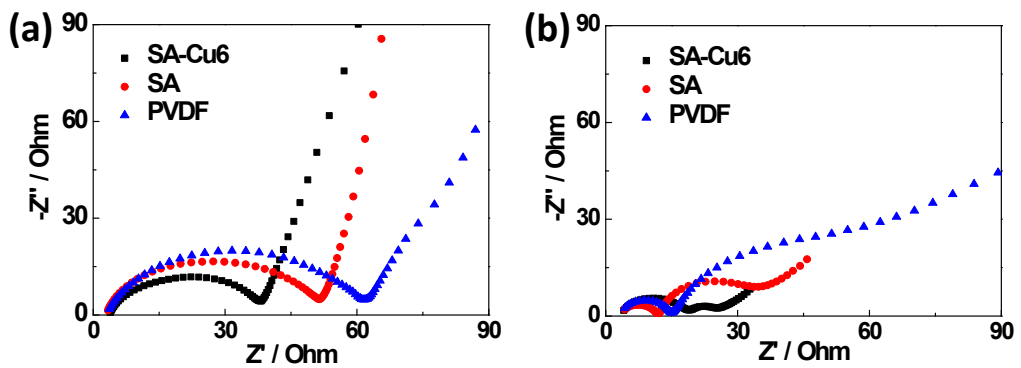


Fig. S6 (a) EIS of fresh cells and (b) cells after 20 cycles at 0.2 C fabricated with different binders.

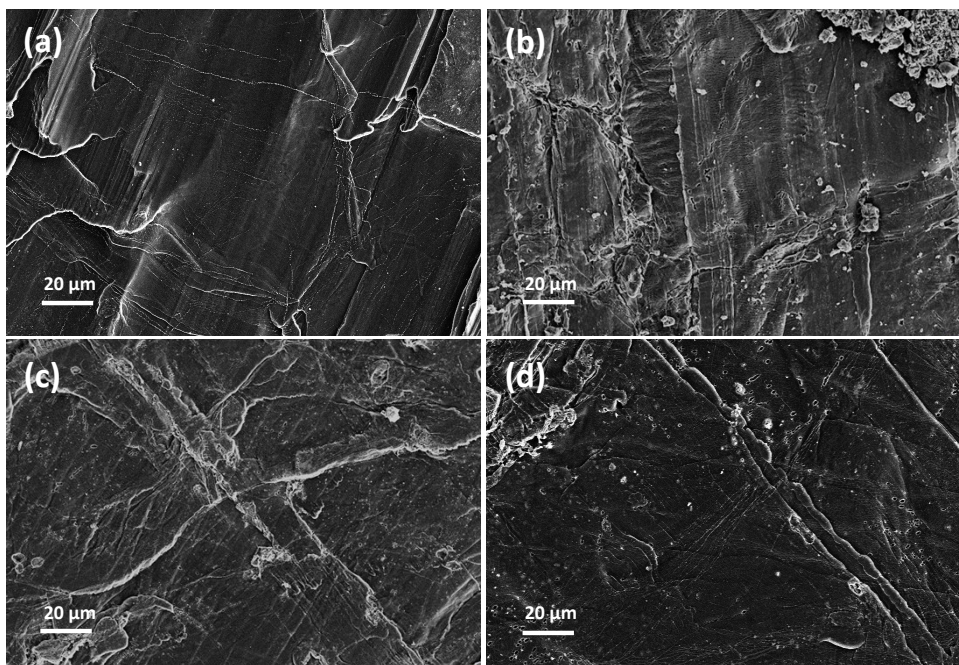


Fig. S7 SEM images of (a) fresh lithium foil anode and lithium foil anodes detached from cells fabricated with (b) S@PVDF electrode, (c) S@SA electrode, and (d) S@SA-Cu6 electrode after 20 cycles at 0.2 C.

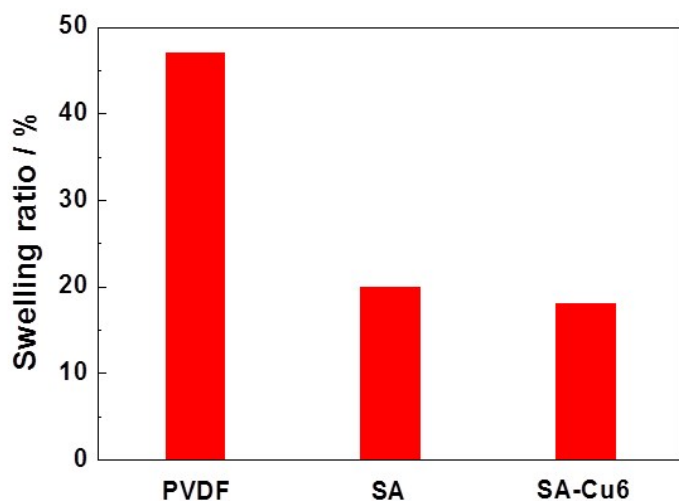


Fig. S8 Swelling ratios of different binders. The swelling ratio is defined as the percent of the increased weight of binder after soaking in the electrolyte for 24 h and the initial weight of binder.

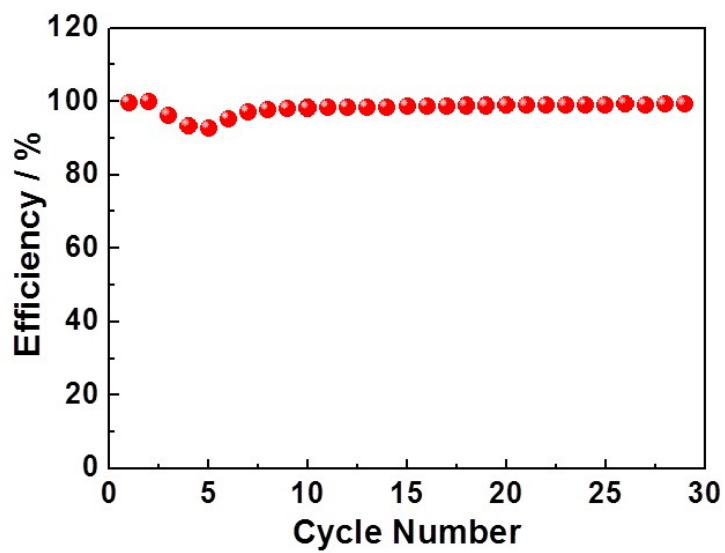


Fig. S9 Coulombic efficiency of high-loading S@SA-Cu6 electrode with a sulfur loading of 8.05 mg cm^{-2} .

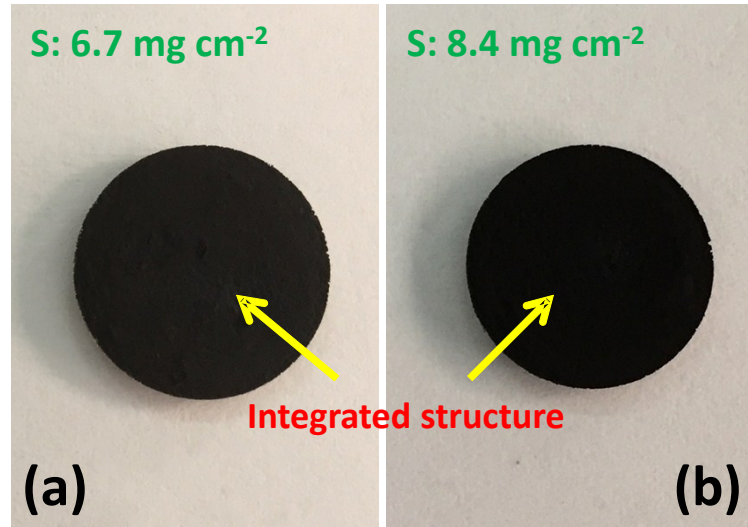


Fig. S10 Photos of high-loading S@SA-Cu6 electrodes with sulfur loadings of (a) 6.7 and (b) 8.4 mg cm^{-2} showing the crack-free electrode structure. The electrodes consist of S/super P composite and SA-Cu6 binder without 1D and 2D carbon materials.